Desalination and Water Treatment
www.deswater.com

doi: 10.5004/dwt.2022.28727

269 (2022) 228–237
September

Hydrodynamics analysis and coordinated control method of anti-lock brake based on dynamic axle load

Libin Zhang[a], Qifeng Liu[a,*], Hongying Shan[b], Dao Wu[a]

[a]*College of Transportation, Jilin University, Changchun 130025, China, email: q18098809@163.com (Q. Liu)*
[b]*School of Mechanical and Aerospace Engineering, Jilin University, Changchun 130025, China*

Received 11 June 2021; Accepted 18 July 2022

ABSTRACT

In order to improve the stability of anti-lock braking process, a dynamic analysis and coordinated control method of anti-lock brake based on dynamic axle load is proposed. On the basis of dynamic axle load, the wheel force of vehicle braking on hard road is analyzed according to the total resistance of vehicle driving, and the dynamic analysis of vehicle hydraulic braking process is completed based on hydrodynamics theory. The coordinated control model of hydraulic anti-lock braking system is established by using the difference equation of motion of hydraulic anti-lock braking system. The experimental results show that the control method can reduce the braking distance and improve the stability of the braking process.

Keywords: Dynamic axle load; Automobile hydraulic pressure; Anti-lock braking; Coordinated control; Theory of fluid mechanics

1. Introduction

The braking performance of automobile is one of the important performance of automobile, which is directly related to the driving safety of automobile [1]. At the same time, good braking performance is also the premise to improve the speed of the car. Without good and reliable braking performance as a guarantee, the high-speed driving of the car will be impossible [2]. As a driving assistant system, anti-lock braking system can avoid wheel lock and ensure driving safety under emergency braking conditions, which is an essential device in every vehicle [3,4]. With the rapid development of automobile industry, more and more new technologies, especially electronic technology, have been applied to automobile brake system. For example, ABS (Anti-lock Braking System), EBD (Electric Brake Force Distribution) and ESP (Electronic Stability Program) have become the standard configuration of modern vehicles. ABS can improve the handling stability and shorten the braking distance in the process of automobile braking, so as to effectively guarantee the safety of automobile. It is the first way to improve the active safety of automobile, and it has become the necessary configuration on passenger vehicles [5,6].

Ahn et al. [7] believe that automobile braking and steering system is the most effective actuator that directly affects the dynamic performance of automobile. Generally speaking, the braking system affects the longitudinal dynamics and the steering system affects the lateral dynamics; however, when the vehicle is braked on a non-uniform surface, their effects are coupled. Yaw moment compensation of multi branch steering control is one of the basic functions of integrated or coordinated chassis control system, which has been proved by many chassis suppliers. However, the disturbance yaw moment is usually compensated by yaw rate feedback or wheel brake pressure measurement. It is not cost-effective to obtain the wheel brake pressure through physical sensors; therefore, this paper models the hydraulic brake system to avoid using physical sensors and estimate the brake pressure. The steering angle controller is designed to reduce the influence of asymmetric braking force and stabilize the yaw rate dynamics of the vehicle. Han et al. [8]

* Corresponding author.

introduced a control method of anti-lock braking system (ABS) for electric vehicles. The non-linear characteristic of tire force is used to solve the problem of vehicle skidding. The front wheel uses the motor as the actuator instead of the traditional front wheel hydraulic brake system, and the rear wheel is still controlled by the hydraulic system. The effectiveness of the method is verified by simulation and real vehicle experiment [9].

In order to study the coordinated control of the hydraulic anti-lock braking system, the control system designed in this paper focuses on the coordinated control of the vehicle body subsystem, and focuses on solving the coupling problem between the steering system and the braking system when the vehicle is steering and braking. In the design of automobile steering control system, active front wheel control and yaw moment control are used to calculate the front and rear wheel side slip characteristic parameters on line, and adjust the steering control amount by itself. In the design of automobile longitudinal brake, the coordination error is defined, the compensation controller is added, the vertical load of wheel is calculated on line, and the brake control amount is calculated by self-adjusting correction. The coordination controller can dynamically compensate the interference of steering control to the longitudinal braking, and make the whole system have good real-time, stability and coordination. Each error decays to zero with the same attenuation rate. Under the control of the coordinated control system, the vehicle state can have both good steering tracking performance and good longitudinal braking performance. The accuracy, real-time, coordination and stability of the tracking trajectory meet the requirements. The effectiveness of the control algorithm is verified by the detailed simulation results [10].

2. Design of coordinated control method for hydraulic anti-lock braking of automobile

2.1. Anti-lock brake process based on fluid dynamics theory

In the normal driving process of the vehicle, gasoline enters the brake through the oil inlet hole, the piston compacts the disc spring group, there is no pressure between the friction plates, the gear shaft is free to idle by driving the internal friction plate. Brake solenoid valve power reset, brake cavity and oil pool connection, disc spring drive piston, press internal and external friction plate, play the role of braking vehicle. Therefore, the anti-lock braking process analysis based on hydrodynamic theory. When driving on a horizontal road, the wheels need to overcome the rolling resistance from the ground, and the vehicle body needs to overcome the air resistance from the air [11–13]; when driving on a ramp, the vehicle must also overcome the slope resistance; when accelerating, the vehicle needs to overcome the acceleration resistance. Therefore, the total resistance of vehicle driving is:

$$\sum F = F_f + F_w + F_i + F_j \tag{1}$$

where F_f is rolling resistance; F_w is air resistance; F_i is slope resistance; F_j is acceleration resistance.

The calculation of each resistance is shown in Eqs. (2)–(7):

Rolling resistance:

$$F_f = \mathrm{mg}f\cos\alpha \tag{2}$$

$$f = f_0 + f_1\left(\frac{v_a}{100}\right) + f_4\left(\frac{v_a}{100}\right)^4 \tag{3}$$

Air resistance:

$$F_w = \frac{C_D A}{21.15} v_a^2 \tag{4}$$

Slope resistance:

$$F_i = \mathrm{mg}\sin\alpha \tag{5}$$

Acceleration resistance:

$$F_j = \delta m\frac{dv_a}{dt} \tag{6}$$

$$\delta = 1 + \frac{1}{m}\frac{\sum I_w}{r^2} + \frac{1}{m}\frac{I_f i_g^2 i_0^2 \eta_T}{r^2} \tag{7}$$

where m represents the vehicle curb weight, g represents the acceleration of gravity, f represents the coefficient of rolling resistance, α represents the angle of road slope, C_D represents the coefficient of air resistance, A represents the windward area, v_a represents the speed, δ represents the conversion coefficient of vehicle rotating mass, I_w represents the moment of inertia of wheel, r represents the rolling radius of wheel, I_f represents the moment of inertia of flywheel, i_g represents the speed ratio of gearbox, i_0 represents the speed ratio of main reducer, η_T is the total efficiency of the driveline [14].

In the process of automobile braking, the force opposite to the driving direction is not only the external resistance, but also the braking force provided by the braking system. The wheel is mainly affected by three forces: Ground braking force, brake braking force and ground adhesion. Among them, the ground braking force is the external force that makes the car brake and slow down [15]. But the braking force of the ground depends on the friction of two friction pairs: one is the friction between the brake lining and the brake disc of the brake drum, the other is the friction between the tire and the ground, that is, the ground adhesion.

When neglecting the rolling resistance couple moment and the inertia force and inertia force couple moment when decelerating, the wheel force of the car when braking on a good hard road surface is shown in Fig. 1.

In Fig. 1 F_b represents the ground braking force, T_u represents the braking torque, r represents the wheel radius, W represents the vertical load of the wheel, U_a represents the speed of the vehicle, and F_z represents the normal force of the ground on the wheel [16].

According to the torque balance relationship, the brake force is as follows:

$$F_u = \frac{T_u}{r} \tag{8}$$

The braking force is only related to the structural parameters of the brake, that is, its size depends on the type of the brake disc or drum), the structural size, the acting area, the friction factor, etc., and is directly proportional to the air pressure of the brake cylinder of the corresponding wheel.

2.2. Build the coordinated control model of hydraulic anti-lock brake

The vehicle is a complex multi degree of freedom space motion system. If all degrees of freedom are considered, a corresponding number of motion differential equations must be listed, which will make the analysis and solution extremely difficult, and the vehicle parameters required are many and most of them are not easy to measure accurately, the operability is poor, and the interference of some secondary factors will often reduce the simulation accuracy. On the contrary, it cannot highlight the nature and characteristics of the problem [17].

In the process of modeling, the origin of vehicle coordinate system coincides with the center of mass of the vehicle, and the vehicle coordinate system fixed on the vehicle is used to describe the movement of the vehicle.

By analyzing the motion of the system and applying Newton's law, the differential equation of the system can be derived as follows:

Vehicle lateral motion equation:

$$m\left(v_y + \gamma v_x\right) = F_{yf}\cos\delta + F_{yr} - F_{xf}\sin\delta \tag{9}$$

Equation of motion of yaw:

$$I_z\gamma = aF_{yf}\cos\delta - bF_{yr} - aF_{xf}\sin\delta \tag{10}$$

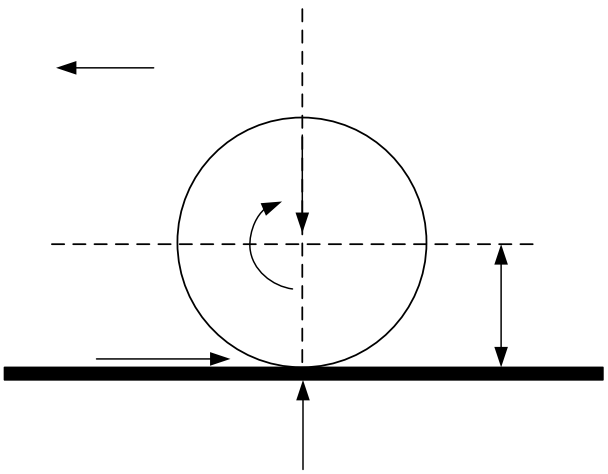

Fig. 1. Wheel braking force analysis.

Equation of longitudinal motion:

$$m\left(v_x - \gamma v_y\right) = -\left(F_{\mathrm{xr}} + F_{\mathrm{xf}}\cos\delta + F_{\mathrm{yf}}\sin\delta\right) \tag{11}$$

Rotation equation of front wheel:

$$I_f\omega_f = F_{\mathrm{xf}}R_f - \mathrm{T_{bf}} \tag{12}$$

Equation of rear wheel rotation:

$$I_r\omega_r = F_{\mathrm{xr}}R_r - T_{\mathrm{br}} \tag{13}$$

where m represents the mass of the whole vehicle, m represents the speed of the vehicle in the driving direction, v_x represents the longitudinal speed of the vehicle, v_y represents the transverse speed of the vehicle, γ represents the angular speed of the vehicle, I_f and I_r represent the rotational momentum of the front and rear wheels, ω_f and ω_r represent the angular speed of the front and rear wheels, F_{xf} and F_{xr} represent the longitudinal force of the front and rear tires, F_{yf} and F_{yr} represent the transverse force of the front and rear tires, a and b represent the centroid distance of the front and rear wheels.

2.3. Design the coordinated control strategy of vehicle hydraulic anti-lock system

In the process of anti-lock braking, the coordinated control of regenerative braking and hydraulic braking is the focus of the research of electric vehicle braking system. As shown in Fig. 2, after the anti-lock control algorithm completes the road identification, different coordinated control

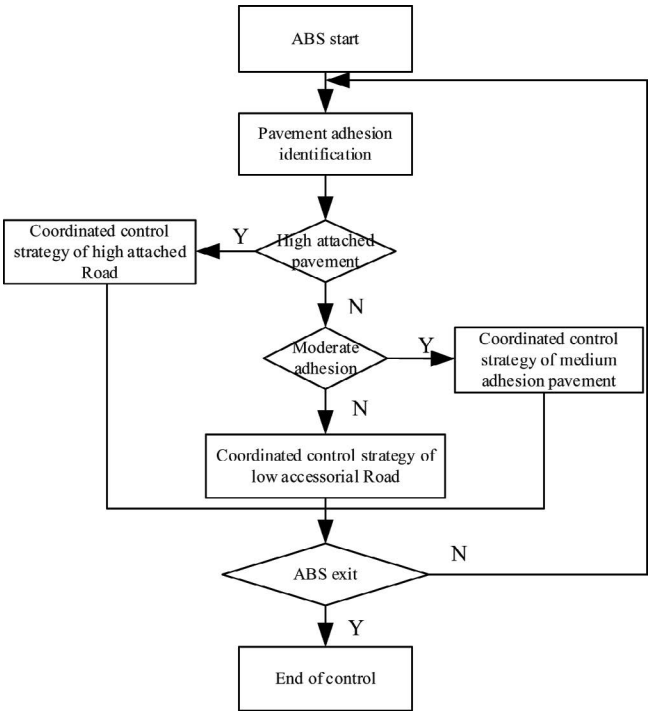

Fig. 2. Anti-lock control flow chart.

methods are adopted according to the road conditions [18]. In the control process, the road adhesion coefficient is always identified. When the adhesion coefficient changes, the control strategy is switched.

On the low attachment Road, the foundation pressure is provided by the hydraulic braking system, and the motor is used for anti-lock adjustment. On the low adhesion road, the wheels are easy to lock up, and the slight change of braking force may cause the sharp change of wheel speed. Because of the precise control and quick response of the motor, the anti-lock control of the motor can improve the control accuracy and control effect. At the same time, considering the maximum braking energy recovery capacity of the motor and battery, the hydraulic system provides the basic pressure, which is of great significance to eliminate the gap and improve the quick response of ABS after the motor failure [19].

On the medium adhesion road, anti-lock adjustment is carried out by the hydraulic actuator, and the motor provides basic braking. The traditional ABS controller can only divide the road into high adhesion and low adhesion. The distributed drive vehicle studied in this paper can obtain the regenerative braking torque and wheel cylinder pressure of the motor, so it can effectively estimate the road adhesion. Taking specific strategies for the anti-lock control on the medium adhesion road can improve the control effect. Considering that the braking torque will fluctuate greatly in the process of anti-lock control of medium adhesion road, and the current motor regenerative braking capacity is small, which cannot meet the requirements of slip rate control, so the regenerative braking torque is taken as the basic torque, and the wheel slip rate is controlled through the adjustment of hydraulic braking force [20]. In this process, when the motor works at the maximum or larger regenerative braking torque, it is beneficial to improve the energy recovery efficiency in the process of anti-lock control.

On the high attached road, after entering the anti-lock braking control, the regenerative braking gradually exits, and the anti-lock control is completed by the hydraulic braking. Because the stability is the primary control objective in the process of anti-lock control on the high adhesion road, the traditional anti-lock control method of hydraulic braking is relatively mature, so the motor regenerative braking is withdrawn, and the hydraulic braking completely completes the slip rate control. In previous studies, after ABS is started, regenerative braking is usually cancelled directly or reduced to 0 at a certain rate. In this process, hydraulic braking is used to compensate for the reduction of regenerative braking [21–23]. Direct cancellation of regenerative braking, if the proportion of regenerative braking in the total braking is relatively large, it is easy to cause ABS to exit and start frequently, and gradually reduce the regenerative braking. Due to the need to use hydraulic compensation to reduce the amount, there is a high demand for hydraulic control accuracy.

3. Comparative analysis of experiments

3.1. Simulation condition analysis

Because there is no corresponding standard for the control method studied in this paper, RBS or ABS standard is considered as the reference of simulation conditions. At present, there is no unified standard for dynamic axle load system, while the national standard GB/T13594-2003 is used as the unified standard for anti-lock braking system. Therefore, the simulation conditions and working conditions of this paper are set according to the relevant conditions in GB/T13594-2003. The experimental conditions selected in this paper are as follows: at the initial speed of 60 and 120 km/h, the full force braking is accelerated. Working conditions: high adhesion road and low adhesion road. The initial SOC value of the battery is 60%. The pavement with high adhesion coefficient is 0.8, and the pavement with low adhesion coefficient is 0.2. It meets the conditions of $k_H \geq 0.5$ and $k_H/k_l \geq 2$.

In this paper, the control strategy of the vehicle hydraulic anti-lock brake coordination control model on the open circuit surface is that the front and rear axles adopt the low selection control strategy, that is, on the open circuit surface, when the low adhesion side wheel triggers the vehicle hydraulic anti-lock brake coordination control model and the high adhesion side wheel has not yet triggered the vehicle hydraulic anti-lock brake coordination control. The whole system also needs to enter the model control of vehicle hydraulic anti-lock brake coordination control. In this case, the control strategy of the coordinated control model of the vehicle hydraulic anti-lock braking takes the threshold value of the low adhesion side as the actual operation threshold value. Because of this control strategy, the simulation results of the split road are consistent with those of the low adhesion road. In order to save the space of the paper, the simulation results of split road will not appear in the following simulation results. The simulation results of low adhesion road surface can be used to represent the simulation results on the open road surface [24].

3.2. Evaluation index analysis

Evaluation index is a quantitative standard used to evaluate the algorithm. For RBS and ABS coordinated control, there is no definite evaluation index at present. In this paper, the evaluation index of RBS and ABS coordinated control algorithm is studied.

The main function of hydraulic anti-lock braking system is to recover braking energy. It can be seen from previous scholars' research that the energy charged into the battery can well evaluate the advantages and disadvantages of the vehicle hydraulic anti-lock braking system, and the energy charged into the battery can be quantified by the SOC of the battery, so SOC should be one of the evaluation indexes of this algorithm [25].

For the anti-lock braking system, the main evaluation indexes include the braking distance of the vehicle, the steer ability during braking, etc. The steer ability during braking can be evaluated by whether the wheels are locked or not, and the braking distance itself is an evaluation index. The standard of whether the wheel is locked or not can be in accordance with the provisions of GB /T13594-2003, "the wheel is allowed to lock temporarily, and when the speed is lower than 15 km/h, the wheel is also allowed to lock."

To sum up, the evaluation indexes of this paper are: SOC of battery, wheel locking, braking distance of vehicle.

3.3. Simulation results

According to the anti-lock control flow of vehicles shown in Fig. 2, the simulation results of high viscosity pavement at different initial speeds are analyzed.

3.3.1. Simulation results of high adhesion pavement

(1) Simulation results at initial speed of 60 km/h:

For the first control strategy, the control algorithm for fully withdrawing the motor braking torque after ABS triggering is shown in the simulation results in Fig. 3.

It can be seen from Fig. 3a and b that the coordinated control strategy has little effect on the control effect of ABS. When the wheel speed is more than 2 m/s, there is a process of separation and recovery, and the front and rear axle slip rates fluctuate near the optimal slip rate, achieving the purpose of ABS control. After 2 m/s, ABS exits the control,

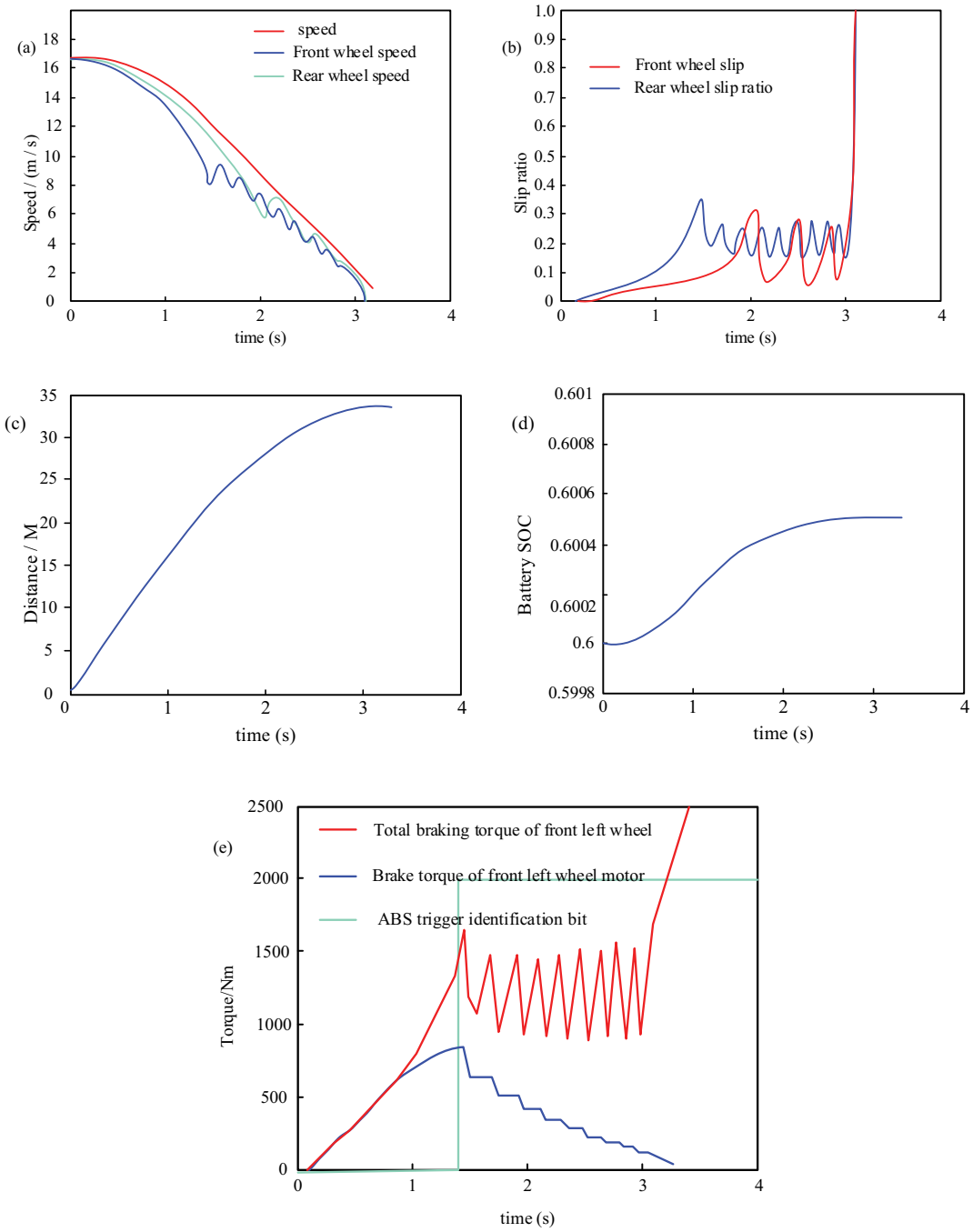

Fig. 3. Simulation result curve of the control method in this paper under the condition of low speed and high attachment. (a) Speed and wheel speed, (b) slip ratio, (c) braking distance, (d) battery SOC, and (e) left front wheel hydraulic and motor braking torque.

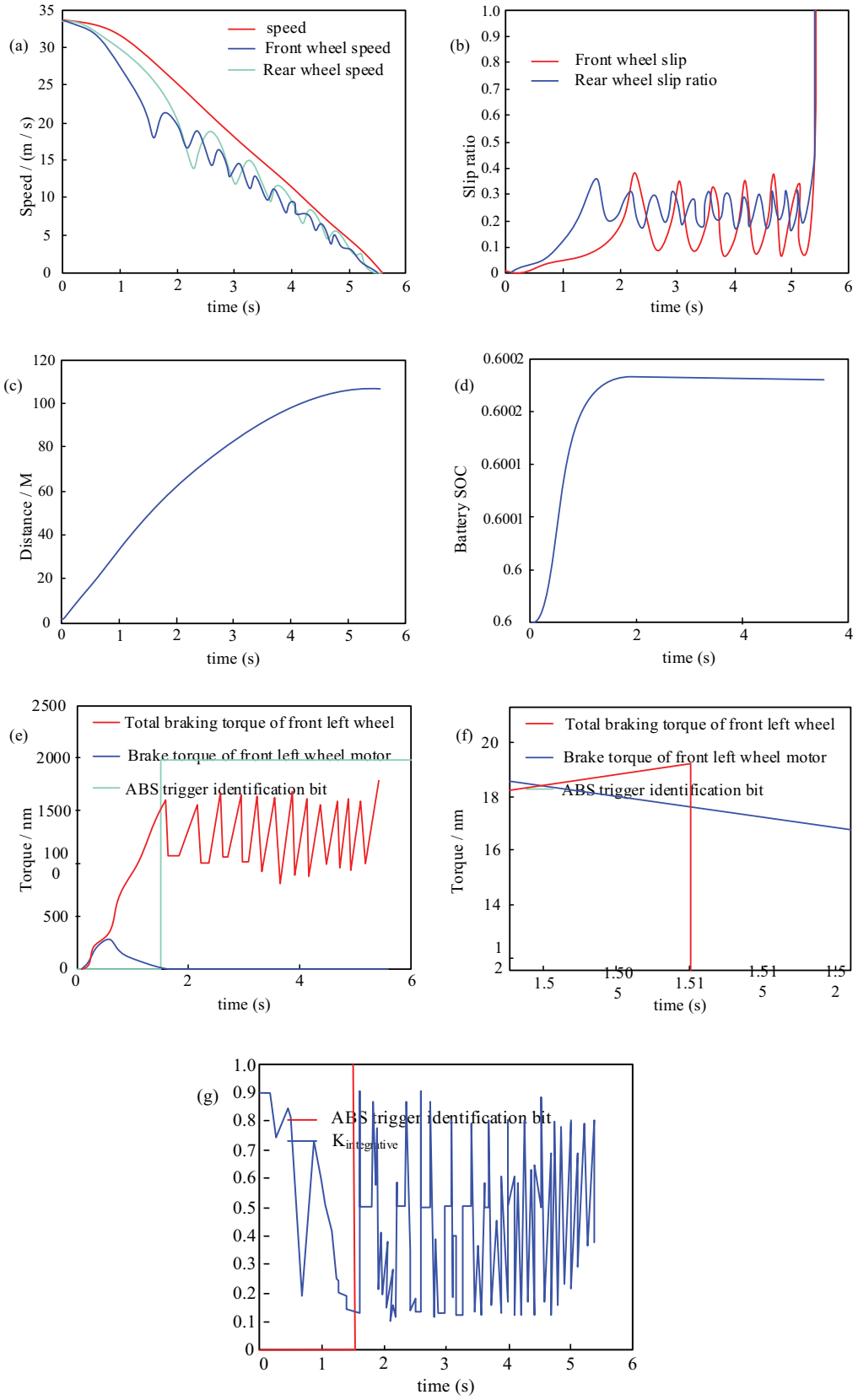

Fig. 4. Simulation result curve of coordinated control method undertable high speed and high attachment conditions. (a) Speed and wheel speed, (b) slip ratio, (c) braking distance, (d) battery SOC, (e) left front wheel hydraulic and motor braking torque, (f) enlarged drawing of brake torque of front left wheel motor, and (g) $K_{integrative}$ and ABS trigger flag bits.

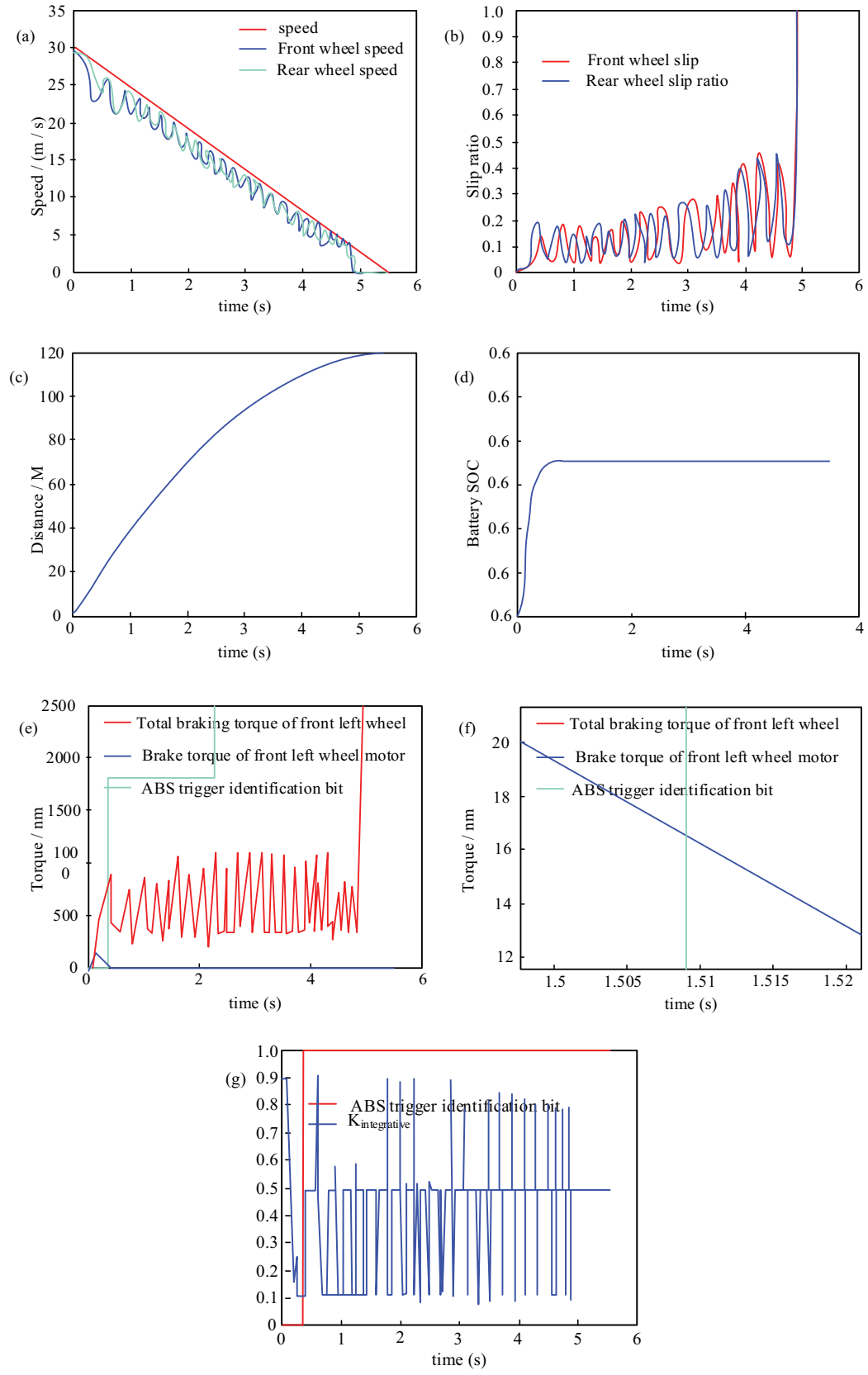

Fig. 5. Simulation result curve of the control method in this paper under low speed and low attachment conditions. (a) Speed and wheel speed, (b) slip ratio, (c) braking distance, (d) battery SOC, (e) left front wheel hydraulic and motor braking torque, (f) enlarged drawing of brake torque of front left wheel motor, and (g) $K_{integrative}$ and ABS trigger flag bits.

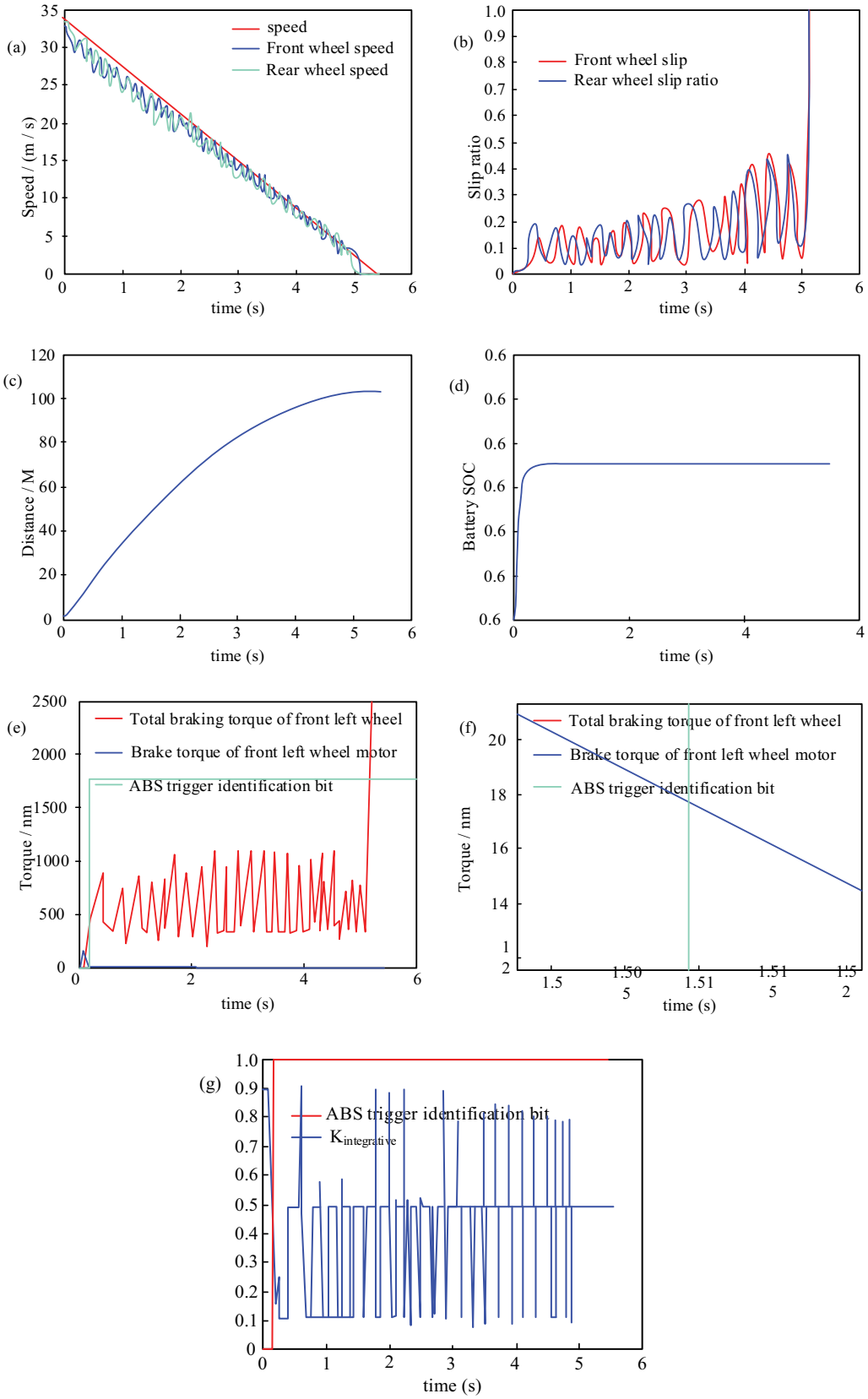

Fig. 6. Simulation result curve of coordinated control method under high speed and low attachment conditions. (a) Speed and wheel speed, (b) slip ratio, (c) braking distance, (d) battery SOC, (e) left front wheel hydraulic and motor braking torque, (f) enlarged drawing of brake torque of front left wheel motor, and (g) $K_{integrative}$ and ABS trigger flag bits.

and the wheels lock until they stop. Fig. 3e shows that the coordinated control method is well executed. Before ABS triggering, the motor braking torque is executed according to RBS algorithm, and after ABS triggering, the motor braking torque step decreases [26].

The braking distance and battery SOC shown in Fig. 3c and d are the quantitative evaluation indexes in this paper. The braking distance of this braking process is 33.84 m, and the SOC of battery increases by 0.05%.

Due to the large lag in the process of motor exit, the actual torque value is slower than the control signal, resulting in the increase of decompression time. Reflected in the braking distance is the increase of braking distance. At the same time, since the braking torque of the motor decreases until 0 after the ABS is triggered, the energy recovered by regenerative braking decreases and remains unchanged at last.

(2) The simulation results at the initial speed of 120 km/h are shown in Fig. 4.

The braking torque of the motor is about 18 nm when ABS is triggered, and the total braking torque of the wheel compared with 1,500 nm can be ignored.

The braking distance of the control method in this paper is 106.8 m, and the SOC of the battery increases by 0.02%. Because the motor is less involved in the braking process, the frequent conversion of different braking systems is reduced, thus the braking distance is increased. This control algorithm is almost the same as the second-one in the index of braking distance. However, because the motor is less involved in the braking process, the proposed method is greatly reduced in the SOC index of battery.

3.3.2. Simulation results analysis of low adhesion pavement

(1) The simulation results at the initial speed of 60 km/h are shown in Fig. 5.

When ABS is triggered, the residual torque of the motor is shown in Fig. 5f, about 20 nm. The braking torque of the wheel at this time is 400 nm, about 5%, which meets the engineering requirements [27,28].

The braking distance of the control method in this paper is 79.33 m, and the SOC of the battery increases by 0%. The reason for almost no increase of SOC in battery is that in the case of emergency braking on low adhesion road, the intervention of coordinated control algorithm affects the RBS effect very early, and the motor does not recover energy in the process of ABS braking.

(2) The simulation results at the initial speed of 120 km/h are shown in Fig. 6.

When ABS is triggered, the residual torque of the motor is shown in Fig. 6f, about 9 nm. The total braking torque of the wheel at this time is 400 nm, about 2%, which meets the engineering requirements.

The braking distance of the control method in this paper is 304.5 m, and the SOC of the battery increases by 0%.

Above, the control method of this paper is simulated under different road surface and different vehicle speed. The results prove the effectiveness of the method, and analyze the respective effects and influencing factors. Then, according to the braking distance and SOC results of battery, the three control strategies are analyzed comprehensively [29].

Table 1
Braking distance of the control method in this paper under different simulation conditions

Pavement	Low speed	High speed
High attached pavement	33.22 m	106.8 m
Low adhesion pavement	79.33 m	304.5 m

In order to verify the braking distance of the control method in this paper more intuitively, the braking distance of the method in this paper under different simulation conditions is drawn as Table 1.

The coordinated control method based on dynamic axle load has the change of motor braking torque, but because the motor braking torque has been limited before ABS triggering, the motor braking torque which responds slowly after ABS triggering exits the braking process, so it does not affect the ABS braking process, and the braking distance is relatively small.

4. Conclusion

In this paper, a method of hydrodynamics analysis and coordinated control of anti-lock brake based on dynamic axle load is proposed. The results show that the coordinated control method can reduce the braking distance to ensure the safety of the vehicle in the process of driving, whether it is applied to high or low adhesion road. But in the design of coordinated control method, the analysis of road friction should be added to avoid the influence of external factors.

References

[1] A.I. Bondarenko, I.O. Taran, Effect of antilock brake system on basic parameters of transport vehicle transmission, Naukovyi Visnyk Natsionalnoho Hirnychoho Universytetu – Min. Mech., 2 (2017) 75–80.
[2] D. Savitski, V. Ivanov, B. Shyrokau, T. Pütz, J. De Smet, J. Theunissen, Experimental investigations on continuous regenerative anti-lock braking system of full electric vehicle, Int. J. Automot. Technol., 17 (2016) 327–338.
[3] T. Köppen, T. Küpper, O. Makarenkov, Existence and stability of limit cycles in control of anti-lock braking systems with two boundaries via perturbation theory, Int. J. Control, 90 (2017) 974–989.
[4] R. Verma, D. Ginoya, P.D. Shendge, S.B. Phadke, Slip regulation for anti-lock braking systems using multiple surface sliding controller combined with inertial delay control, Veh. Syst. Dyn., 53 (2015) 1150–1171.
[5] B.H. Sababha, Y.A. Alqudah, A reconfiguration-based fault-tolerant anti-lock brake-by-wire system, ACM Trans. Embedded Comput. Syst., 17 (2018) 1–13.
[6] S.L. Perić, D.S. Antić, M.B. Milovanović, D.B. Mitić, M.T. Milojković, S.S. Nikolić, Quasi-sliding mode control with orthogonal endocrine neural network-based estimator applied in anti-lock braking system, IEEE/ASME Trans. Mechatron., 21 (2016) 754–764.
[7] C. Ahn, B. Kim, M. Lee, Modeling and control of an anti-lock brake and steering system for cooperative control on split-mu surfaces, Int. J. Automot. Technol., 13 (2012) 571–581.

[8] K. Han, B. Lee, S.B. Choi, Development of an antilock brake system for electric vehicles without wheel slip and road friction information, IEEE Trans. Veh. Technol., 68 (2019) 5506–5517.
[9] C. Feng, Key technologies of low carbon design integrated system for typical automobile parts, J. Comput. Methods Sci. Eng., 19 (2019) S115–S122.
[10] A.K. Singh, I. Nasiruddin, A.K. Sharma, A. Saxena, Modelling, analysis and control of an eddy current braking system using intelligent controllers, J. Intell. Fuzzy Syst., 36 (2019) 2185–2194.
[11] W. Sun, J. Zhang, Z. Liu, Two-time-scale redesign for antilock braking systems of ground vehicles, IEEE Trans. Ind. Electron., 66 (2018) 4577–4586.
[12] J. Zhang, W. Sun, H. Jing, Nonlinear robust control of antilock braking systems assisted by active suspensions for automobile, IEEE Trans. Control Syst. Technol., 27 (2019) 1352–1359.
[13] M. Corno, F. Roselli, L. Onesto, F. Molinaro, E. Graves, A. Doubek, S.M. Savaresi, Experimental validation of an antilock braking system for snowmobiles with lateral stability considerations, IEEE Trans. Control Syst. Technol., 28 (2018) 705–712.
[14] S.G. Song, X.P. Li, D.P. Margaris, Electric vehicle electric-hydraulic regenerative braking strategy based on variable current feedback, J. Mech. Eng. Res. Dev., 39 (2016) 403–412.
[15] A. Patil, D. Ginoya, P.D. Shendge, S.B. Phadke, Uncertainty-estimation-based approach to antilock braking systems, IEEE Trans. Veh. Technol., 65 (2016) 1171–1185.
[16] Y. Chen, J. Li, H. Lu, P. Yan, Coupling system dynamics analysis and risk aversion programming for optimizing the mixed noise-driven shale gas-water supply chains, J. Cleaner Prod., 278 (2021) 123209, doi: 10.1016/j.jclepro.2020.123209.
[17] F. Guo, S. Wu, J. Liu, Z. Wu, S. Fu, S. Ding, A time-domain stepwise fatigue assessment to bridge small-scale fracture mechanics with large-scale system dynamics for high-speed maglev lightweight bogies, Eng. Fract. Mech., 248 (2021) 107711, doi: 10.1016/j.engfracmech.2021.107711.
[18] O. Makarenkov, Existence and stability of limit cycles in the model of a planar passive biped walking down a slope, Proc. R. Soc. Math. Phys. Eng. Sc., 476 (2020) 62–82.
[19] J.H. Tang, K.Y. Wang, S.Y. Bei, M.M. Sousa, Research on braking force distribution strategy of composite braking system of hybrid electric vehicle, J. Mech. Eng. Res. Dev., 39 (2016) 373–386.
[20] A. Manivanna Boopathi, A. Abudhahir, Adaptive fuzzy sliding mode controller for wheel slip control in antilock braking system, J. Eng. Res., 4 (2016) 18–26.
[21] H. Chen, G. Zhang, D. Fan, L. Fang, L. Huang, Nonlinear Lamb wave analysis for microdefect identification in mechanical structural health assessment, Measurement, 164 (2020) 108026, doi: 10.1016/j.measurement.2020.108026.
[22] Y. Wang, L. Cao, P. Hu, B. Li, Y. Li, Model establishment and performance evaluation of a modified regenerative system for a 660 MW supercritical unit running at the IPT-setting mode, Energy, 179 (2019) 890–915.
[23] F. Wang, X.B. Fan, K. Jin, Y.K. Sun, An optimization control of automobile anti-lock braking system based on road condition identification, Comput. Simul., 34 (2017) 155–160.
[24] T.-L. Le, Intelligent fuzzy controller design for antilock braking systems, J. Intell. Fuzzy Syst., 36 (2019) 3303–3315.
[25] S. Yang, X. Wan, K. Wei, W. Ma, Z. Wang, Silicon recovery from diamond wire saw silicon powder waste with hydrochloric acid pretreatment: an investigation of Al dissolution behavior, Waste Manage. (Elmsford), 120 (2021) 820–827.
[26] Y. Zha, G. Liu, F. Ma, R. Guo, Acceleration slip regulation control for four-wheel independently drive electric vehicle based on fuzzy control, J. Comput. Methods Sci. Eng., 20 (2020) 1265–1278.
[27] Y.J. Zheng, Y. Feng, S. Joshi, Construction and study of multi-DOF automobile dynamic model, J. Mech. Eng. Res. Dev., 39 (2016) 187–196.
[28] K. Zhang, M.H. Shalehy, G.T. Ezaz, A. Chakraborty, K. Mushfique Mohib, L. Liu, An integrated flood risk assessment approach based on coupled hydrological-hydraulic modeling and bottom-up hazard vulnerability analysis, Environ. Modell. Software, 148 (2022) 105279, doi: 10.1016/j.envsoft.2021.105279.
[29] C. Zhang, J. Ou, Control structure interaction of electromagnetic mass damper system for structural vibration control, J. Eng. Mech., 134 (2008) 428–437.